दुर्घटना सहिष्णु ईंधन आवरण

1

एलओसीए स्थितियों के तहत जिर्केलॉय-4 पर दुर्घटना सहिष्णु ईंधन (एटीएफ) आवरण के रूप में Cr लेपन का विकास और पीएचडब्ल्यूआर की अभिक्रियाशीलता पर लेपन के मोटाई की निर्भरता का प्रभाव

सुबीर कुमार घोष[1]*, सतीश सी. मिश्रा[1], वी.एस.वी. अनंथा कृष्णा[2], विशाल सिंह[2], सुप्रतिक रॉयचौधरी[2], अनमोल सिंह[3], वी. हरिकृष्णन[3], उषा पाल[3], आर. कार्तिकेयन[3], के.के. यादव[3], अलोक अवस्थि[1] एवं राघवेंद्र तिवारी[4]

[1]पदार्थ प्रक्रमण एवं संक्षारण अभियांत्रिकी प्रभाग, भाभा परमाणु अनुसंधान केंद्र, ट्रांबे, मुंबई - 400 085, भारत
[2]पदार्थ विज्ञान प्रभाग, भाभा परमाणु अनुसंधान केंद्र, ट्रांबे, मुंबई - 400 085, भारत
[3]रिएक्टर भौतिकी अभिकल्पन प्रभाग, भाभा परमाणु अनुसंधान केंद्र, ट्रांबे, मुंबई - 400 085, भारत
[4]पदार्थ वर्ग, भाभा परमाणु अनुसंधान केंद्र, ट्रांबे, मुंबई - 400 085, भारत

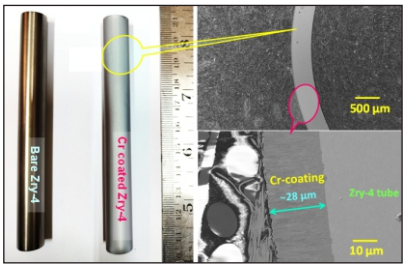

अनावरित और Cr-लेपित Zry-4 ईंधन नलिकाओं की फोटोग्राफिक छायाचित्र और Cr लेपित ईंधन नलिका की एक्स-सेक्शन एफईएसईएम छायाचित्र

सारांश

फुकुशिमा दुर्घटना ने मूल रूप से दुनिया भर के नाभिकीय समुदाय को शीतलक दुर्घटना (डीबीएलओसीए) की स्थिति के अभिकल्पन आधारित हानि को कम करने के लिए लंबे समय से अच्छी तरह से सिद्ध Zr-आधारित आवरण के विकल्पों की खोज करने के लिए मजबूर किया है। दो अलग-अलग अवधारणाएँ-या तो Zr-आधारित आवरण का पूर्ण प्रतिस्थापन या एक उपयुक्त लेपित Zr आधारित आवरण सबसे आशाजनक समाधान के रूप में उभरी है। इस संबंध में, डीसी मैग्नेट्रॉन स्पटरिंग का उपयोग करके जिर्केलॉय-4 (Zr-4) सब्सट्रेट और ईंधन नलिकाओं पर मोटी (20-30 µm), छिद्र-मुक्त अत्यधिक घनी और सुसंगत Cr लेपन को सफलतापूर्वक विकसित किया गया। निक्षेपण के बाद, लेपनों को संरचना, क्रिस्टल संरचनाओं, क्रॉस-सेक्शन माइक्रोस्ट्रक्चर और Zry-4 सब्सट्रेट के साथ आसंजन के संदर्भ में विस्तार से दर्शाया गया। विभिन्न अवधियों के साथ तापमान सीमा 700-1200° C में पूर्ण सतह के Cr लेपित Zry-4 कूपनों और अनावरित Zry-4 के भाप ऑक्सीकरण ने Zry-4 सब्सट्रेट के नीचे के लिए Cr लेपन की उत्कृष्ट सुरक्षा क्षमता का प्रदर्शन किया। 700Mwe पीएचडब्ल्यूआर के 37 पिन समूह में नाभिकीय अभिक्रियाशीलता पर Cr लेपन मोटाई के प्रभाव का विश्लेषण करने के लिए एक सैद्धांतिक जांच की गई। Zry-4 पर 15 µm मोटी Cr लेपन के लिए, यह 7.15% के बर्नअप हानि की संभावना को दर्शाता है। यह अध्ययन इस बात पर प्रकाश डालता है कि डीबीएलओसीए की स्थिति के तहत Zry-4 आवरण की रक्षा के लिए 10-12 µm की सीमा में एक Cr लेपन मोटाई पर्याप्त हो सकती है, जिससे प्रचालन को कोर शीतलन की परिनियोजन के लिए पर्याप्त समय मिल सकता है।

Accident Tolerant Fuel Cladding

1

Development of Cr Coating on Zircaloy-4 as Accident Tolerant Fuel (ATF) Cladding under LOCA Conditions and Coating Thickness Dependent Impact on Reactivity of PHWRs

Subir Kumar Ghosh[1]*, Satish C. Mishra[1], V. S. V. Anantha Krishna[2], Vishal Singh[2], Supratik Roychoudhury[2], Anmol Singh[3], V. Harikrishnan[3], Usha Pal[3], R. Karthikeyan[3], K. K. Yadav[3], Alok Awasthi[1] and Raghvendra Tewari[4]

[1]Materials Processing & Corrosion Engineering Division, Bhabha Atomic Research Centre, Trombay, Mumbai - 400 085, INDIA
[2]Materials Science Division, Bhabha Atomic Research Centre, Trombay, Mumbai - 400 085, INDIA
[3]Reactor Physics Design Division, Bhabha Atomic Research Centre, Trombay, Mumbai - 400 085, INDIA
[4]Materials Group, Bhabha Atomic Research Centre, Trombay, Mumbai - 400 085, INDIA

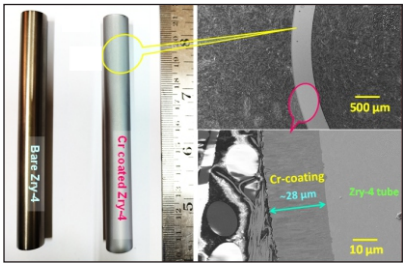

Photographic images of bare and Cr-coated Zry-4 fuel tubes and X-section FESEM images of Cr coated fuel tube

ABSTRACT

Fukushima accident has basically forced world-wide nuclear community to search for alternatives to long served well proven Zr-based claddings to mitigate design basis loss of coolant accident (DB LOCA) condition. Two different concepts- either complete replacement of Zr-based claddings or a suitably coated Zr-base claddings emerged as most promising solutions. In this connection, thick (20-30 µm), pore-free highly dense and adherent Cr coating was successfully developed on zircaloy-4 (Zry-4) substrates and fuel tubes by using DC magnetron sputtering. Post deposition, coatings were characterized in terms of composition, crystal structures, cross-section microstructure and adhesion with Zry-4 substrate in detail. Steam oxidation of full surface Cr coated Zry-4 coupons and bare Zry-4 in the temperature range 700-1200°C with different durations demonstrated excellent protection ability of Cr coating to the underneath Zry-4 substrate. A theoretical investigation was undertaken to analyze the impact of Cr coating thickness on nuclear reactivity in a 37 pin cluster of 700 MWe PHWR. For 15 µm thick Cr coating on Zry-4, it predicts burnup loss of 7.15%. This study highlights that a Cr coating thickness in the range 10-12 µm may be sufficient to protect the Zry-4 claddings under DB LOCA condition allowing sufficient coping time to the operator for restoration of core cooling.

KEYWORDS: Accident Tolerant Fuel (ATF) Cladding, Cr coating, Magnetron Sputtering, LOCA, Steam Oxidation

*Author for Correspondence: Dr. Subir Kumar Ghosh
E-mail: sghosh@barc.gov.in

Introduction

Since the installation of first pressurized reactor named Atomic Power Station-1 (APS-1) at Obninsk (USSR) in the year 1954, zirconium alloys have been selected as cladding and canister materials for UO_2 based fuels because of their very low thermal neutron absorption cross-section, good mechanical properties under neutron irradiation and fairly good oxidation resistance under normal operating conditions [1-3]. It is also well known that at temperatures higher than 450°C, Zr undergo severe oxidation following an exothermic reaction in water/steam environment [4-6]. Past six decades enormous efforts have been put forward to further improve the nuclear fuel performance under normal operating conditions in terms of enhanced fuel burn up for the minimization of waste [7], substantial reduction of fuel failure rates [8-9], increased power density for power upgradation, and extended operational service for economic competitiveness [10]. Despite narrow working temperature range and to meet ever increasing economic power demand without breaching the safety norms and reliability under normal operating conditions of nuclear power plant, several advanced Zr-based alloy claddings, such as Zircaloy-2 (Zry-2), Zircaloy-4 (Zry-4), ZIRLO™, M5, E110, E365, Zr-2.5 Nb, have been developed (Table 1) in a phased manner to mitigate several degradation phenomena such as corrosion (general corrosion, nodular corrosion, galvanic corrosion, shadow corrosion, crud induced localized corrosion), hydriding, debris fretting, cracking due to fission gas accumulation etc. [3,6,11] In fact, Indian PHWRs are also successfully operating safely last few decades utilizing Zry-4 as cladding materials.

Limitations of Zr-based Fuel Claddings

Satisfactory performance, however, of these Zr-based fuel cladding materials are highly challenged once the operation condition breaches the design-basis accident (DBA, 1204°C) and beyond DBA (T>1204°C) scenarios. In the year 2011, accident in Fukushima Daichi Nuclear Power Plant is one such example. A massive earthquake of magnitude 9.0 in Richter scale followed by 15 m tall tsunami severely damaged the reactor building and power supply was disabled leading to complete failure of emergency core cooling system (ECCS).

Due to lack of core cooling and spontaneous fission inside the reactor, the core temperature increased and the cooling water ultimately converted into superheated pressurized steam. As a result, Zr-based cladding suffered high-temperature steam oxidation reaction with release of large amount of hydrogen gas and heat:

$$Zr + 2H_2O\ (g) = ZrO_2 + 2H_2\ (g) + \Delta H \quad (\Delta H = -584.5\ kJ/mol\ at\ 1200^{\circ}C) \quad (1)$$

Significant damage to the reactor building and the consequent release of radioactive fission products were caused by the accumulation of hydrogen gas, which was subsequently burned and exploded [12]. This is a kind of chemical accident rather than nuclear explosion. This is one kind of loss-of-coolant accident (LOCA) in nuclear industry due to fast and strong oxidation during the DBA and beyond DBA (BDBA). LOCA events can be caused by a breakup of the primary cooling system that results in the loss of pressure in the nuclear core and vaporization of the coolant (water/heavy water). Under these conditions, the fuel temperature rises, thereby increasing the porosity of the fuel and resulting in its fragmentation. For example, ~125 kg of Zr metal in PWR reactor could produce 820 MJ of heat and >2.7 kg of H_2 after complete oxidation [4]. Therefore, depending upon a reactor design, several tons of Zr metal present in the reactor core, if fully oxidized, could produce excessive amount of heat and H_2 gas leading to extra burden on ECCS or may lead to explosion.

Table 1: Composition of commercial Zr-based alloys used as claddings in water-cooled nuclear reactors.

Alloy	Nominal Alloy Composition (wt.%)						
	Zr	Sn	Nb	Fe	Cr	Ni	O
Zircaloy-2	Bal.	1.5	-	0.15	0.1	0.05	0.1
Zircaloy-4	Bal.	1.5	-	0.2	0.1	-	-
M5®	Bal.	-	1.0	-	-	-	0.14
ZIRLO™	Bal.	1.0	-	0.1	-	-	0.1
E365	Bal.	1.2	1.0	0.35	-	-	-

Logic behind Accident Tolerant Fuel (ATF) Claddings

Post Fukushima Daiichi incident, primary focus was on to the reduction of burden on ECCS during severe accidental situation. This is a straightforward reason for switching away from Zr-based claddings to an accident tolerant fuel (ATF) cladding. This could be done only by adopting alternative claddings which ultimately decreases the rate of oxidation as well as amount of hydrogen generation due to total oxidation of cladding in the presence of superheated steam. In turn, it will decrease the rate of temperature rise during LOCA condition which ultimately would slower the core degradation process, allowing sufficient time to the operator for coping, and finally reducing the cooling threshold for accident mitigation [13-16]. Therefore, ATF cladding material should be such which can reduce the heating rate as well as total amount of heat generation as a consequence of steam oxidation.

Several investigations revealed that steam at very high temperatures is far more aggressive corrosive media than dry oxygen [17-18]. Fig.1 shows parabolic oxidation behavior of different cladding materials when they are exposed to high temperature steam and the resulting film formed [19-22]. It is evident that the parabolic oxidation rate of zirconia-forming materials has been two to three orders of magnitude higher than that of traditional materials that create protective layers of silica (SiO_2), alumina (Al_2O_3) and chromia (Cr_2O_3). Reduction in oxidation rate of these claddings means decrease in the heating rate and consequently hydrogen generation under severe accidental condition. It is to bring in your notice that ZrO_2 exhibits excellent thermodynamic stability in steam environment retaining its strong adhesion with the base Zr even at T>1100°C [23]. However, it is a very good conductor of oxygen and lacks in protection ability to the underlying Zr metal. Therefore, in order to protect the cladding material from high temperature steam oxidation, the oxide film should be effective barrier for transport of oxidizing species by limiting the solid state diffusion of aggressive species such as H_2O, OH^-, O radical etc. retaining its other physical and chemical stability. Literature has shown that SiO_2, Al_2O_3 and Cr_2O_3 exhibit excellent stability in steam along with effective barrier against diffusion of oxidizing species and other reaction products [24-25]. These oxide films maintain high-temperature oxidation resistance in the order Cr_2O_3<Al_2O_3<SiO_2 with approximately one order of magnitude higher in each.

Considering the thermochemical behavior, all these oxides including ZrO_2 are stable enough at high temperatures because of favorable Gibbs Free Energy [26]. Formation of ZrO_2 and Al_2O_3 from Zr and Al respectively are most stable with very high negative enthalpy of oxidation (ΔH_R) value, followed by SiO_2 and Cr_2O_3 formation associated with significantly less exothermic oxidation of SiC and Cr [27]. It is also pertinent to mention here that volatility of oxides formed at high temperature steam environment is also a matter of concern to many investigators because it might affect the oxidation resistance of the claddings. However, it is now understood that oxide volatility at higher temperature is more relevant for long

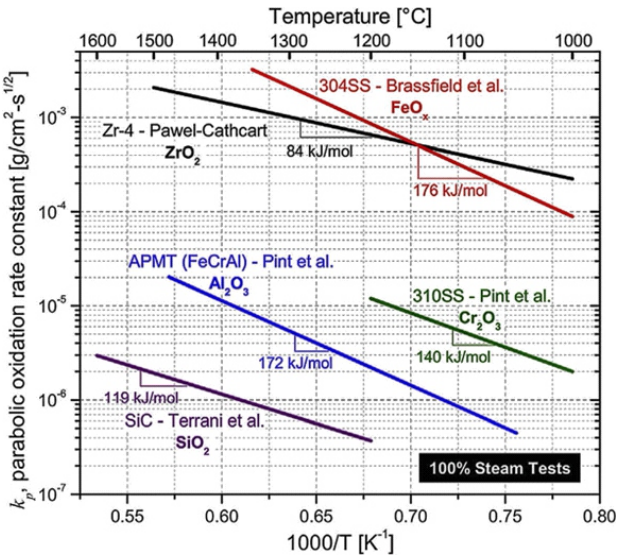

Fig.1: Parabolic oxidation rate of various materials and their corresponding oxides in steam as a function of temperature [19-22].

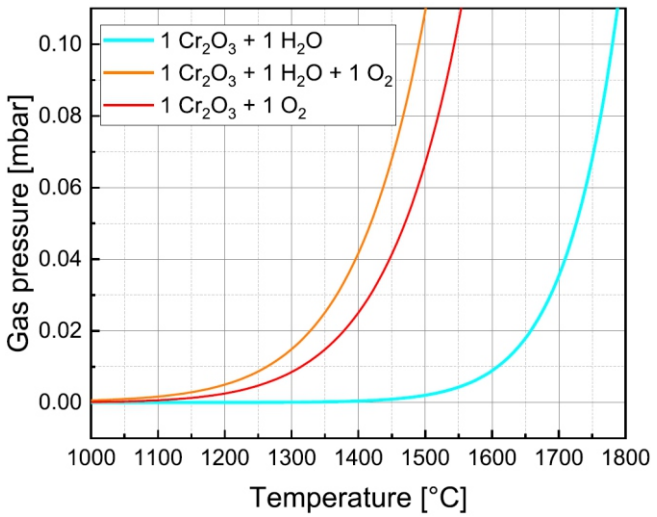

Fig.2: Total gas partial pressure of Cr-containing volatile species over Cr_2O_3 in water, oxygen and mixed atmosphere [26].

exposure times e.g. in turbines, but for accident scenarios such as DB LOCA condition, volatility becomes trivial because of short duration event. Brachet et al [28] confirmed that volatilization of Cr_2O_3 is negligible up to 1300°C in steam atmosphere and the parabolic oxidation rate of Cr in oxygen, air and steam differ significantly, as shown in Fig.2. It is also reported that in pure water vapor oxidation, partial pressure of gaseous Cr-species is 2-3 orders of magnitude lower than O_2 containing atmospheres. This confirms free oxygen is the primary reactant to initiate the oxidation reaction. It is also evident that rapid volatilization of Cr_2O_3 starts in water vapor beyond 1400°C, (conditions similar to short durations LOCA) when other degradation mechanisms become active significantly enough to breach the protective behavior.

Different Concepts of ATF Claddings

Based on the design concept, two main ATF cladding strategies have been considered world-wide.

- One is revolutionary which is to replace the conventional zircaloy based claddings with newer SiC_f / SiC composites [29-32], FeCrAl [4, 33-36], Mo alloys [36-40] etc. This approach is considered as long-term strategy considering involvement of total duration and expenditure for the development of a new type of cladding material.
- The second ATF approach is the development of protective coatings on Zr-based fuel claddings [12,41]. The major advantage of coatings on fuel claddings is to provide significant improvement of oxidation resistance of claddings during LOCA conditions with very little change in original fuel/components design, reactor structure and water chemistry. Therefore, readiness of a suitable coating technology and subsequent incorporation into nuclear fuel fabrication line has been considered as a near-term solution of enhanced ATF cladding.

However, the protective coatings should possess the following criteria:

(i) It should form either Al_2O_3, Cr_2O_3 or SiO_2 oxide layer due to oxidation so that it can provide high temperature oxidation resistance

(ii) Good wear resistance

(iii) Act as barrier for hydrogen absorption of Zr-based claddings

(iv) Preferably low thermal neutron absorption cross-section

(v) Retention of good adhesion with Zr-based cladding during thermal fluctuation

(vi) It should possess good radiation resistance and good heat transfer characteristics

(vii) It should have thermal expansion coefficient very close to Zr-based cladding materials.

Even though the coating technology is comparatively simpler approach, but to meet all these criteria for a given coating/Zr-based cladding under both normal and accident conditions requires enormous research investigations.

Till now, variety of coating materials have been developed to improve Zr-based cladding performance by deposition of pure metallic or alloys [42-53], non-metallic such as nitrides [54-57], carbides [58-59], MAX-phase coatings [12, 60-61]. However, studies have revealed cracking susceptibility of Ti-Al-C and Cr-Al-C MAX-phase coatings during high temperature steam oxidation, water corrosion and thermal cycling [62-63]. On the other hand, SiC coatings undergo corrosion and become unstable at 350°C/20MPa [64]. Also, SiC suffers severely micro-cracking due to its brittleness [10]. Similarly, metal nitride coatings such as CrN undergo decomposition into Cr_2N and N_2 and cracking in the temperature range 500°C to 975°C [65-66]. Considering advantages and disadvantages of various coatings, it is now believed that simple metallic Cr coating might satisfy most of the criteria as a protective coating for Zr-based claddings:

- It provides excellent oxidation resistance to base claddings because of formation of Cr_2O_3 during LOCA. There is wide difference in parabolic oxidation rate of Cr coating and Zircaloy-4 with values 0.05 mg.cm^2.s$^{1/2}$ and 1.09 mg.cm^2.s$^{1/2}$ respectively [23,67].
- Excellent retention of adhesion with Zr-based claddings during quenching of overheated fuel rods like accident condition, after deformation experiments such thermal expansion, ballooning and irradiation induced expansion of fuel tubes under normal operating conditions.
- Because of twice higher elastic modulus of Cr than Zr, the overall stiffness of the claddings gets improved [68].
- Thermal neutron absorption cross-section of Cr (2.9 barns)

Fig.3: Unbalance DC/RF magnetron sputtering system used for Cr coating.

Table 2: Average surface roughness, grain size and mechanical properties of the Cr coating.

Sample	Average Surface Roughness S_a(nm)	Nanohardness (GPa)	Elastic Modulus (GPa)	Average Grain size (nm)
Cr coated Zry-4	268.30±5.80	11.99±0.65	226.86±13.67	19.3±0.5

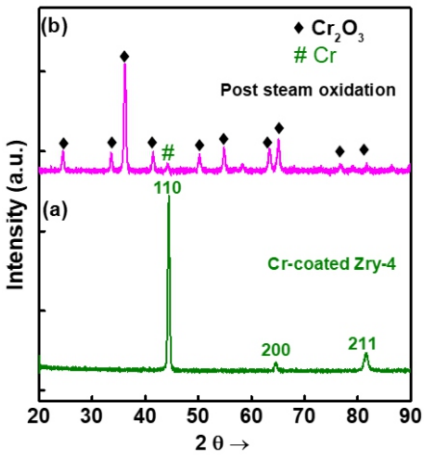

Fig.4: XRD pattern of (a) as deposited Cr coating on Zry-4 substrate and (b) post oxidation of Cr coating.

is comparatively lower in comparison to other competitive coatings.

- Because of higher wettability of Cr than Zircaloy, the thermal-hydraulic performance of the claddings might get improved.
- The eutectic temperature of Cr-Zr (1332^{0}C) is above the DBA temperature (1204^{0}C). The former determines the upper limit of temperature for coatings protection ability during accidental situation [4].

However, in India, development towards ATF fuel claddings either by evolutionary or revolutionary strategies is very limited or absent. In view of these, in the present report, attempts have been made to develop Cr coating on Zry-4 by using magnetron sputtering for protection against superheated steam environment under LOCA condition.

Experimental

Development of Cr Coating on Zry-4

A four target unbalance magnetron sputtering system was used to deposit Cr coating on Zry-4 substrates by employing both DC power source. Prior to deposition the base vacuum achieved was 8.5×10^{-6} mbar and the deposition was conducted at 5×10^{-3} mbar using 99.999% Ar gas. At 250W power, a maximum deposition rate of Cr coating obtained was 5.0±0.1 μm.h^{-1}. As received Zry-4 samples were first cleaned in alkaline solution followed by acid dip in dil. HCl solution and washed in DI water. After cleaning, the coupons were air dried and placed inside the sputtering chamber. Once the base vacuum was achieved, the samples were first subjected to sputter cleaning by applying bias voltage of -400 V. Post sputter cleaning; Cr was deposited on the zircaloy substrate. Fig.3 shows a four target unbalanced magnetron sputtering system used for deposition of Cr coating. For high temperature steam oxidation, Zry-4 coupons of dimension 15 mm x 20 mm were coated with Cr all over the surfaces including edges by flipping the samples. After optimization of sputtering parameters for obtaining thick, dense highly adherent Cr coating, the process was demonstrated on OD surface of Zry-4 fuel tubes of length 100 mm with the help of a four target sputtering system.

Results and Discussions

Characterization of Cr Coating

Deposited coating was smooth, metallic appearance with matte finish and 3D-optical profilometer measurement showed average surface roughness of ~0.2 μm. The nanohardness and elastic modulus of the deposited Cr coating were 11.99±0.65 GPa and 226.86 ±13.67 GPa respectively as given in Table 2.

GIXRD pattern of DC sputtered Cr coated Zry-4 substrate is shown in Fig.4(a) which confirms deposition of crystalline bcc Cr with appearance of (110), (200) and (211) reflections. The XRD pattern was obtained using a Cu$K_{\alpha1}$ X-ray source. Average grain size calculated from XRD peak broadening using Debye-Scherer method was 19.3 nm after subtracting instrumental broadening.

Fig.5(a) represents as-deposited Cr coating top surface morphology consisting of mostly flat but with very small size nodules. Cross-section FESEM investigation confirms sharp Cr/Zry-4 interface without any of gap or voids (Fig.5(b)) indicating integrity of the coating with the substrate. The microstructure along the growth direction exhibits deposition of highly dense coating free from any kind of pores or voids with 20 μm thickness. EDS line scan clearly shows deposition of Cr coating with very sharp composition profile at the interface.

Fig.6(a) displays photograph of bare and highly adherent Cr coated Zry-4 PHWR fuel tubes of 100 mm length and the corresponding X-section image (Fig.6(b)) shows deposition of uniform 28 μm thick Cr coating all across the tubular surface. Fig.6(c) further demonstrates deposition of pore-free, highly adherent Cr coating with columnar grain structure. However, a careful observation shows fine grain equiaxed structures near the coating/substrate interface which gradually transformed

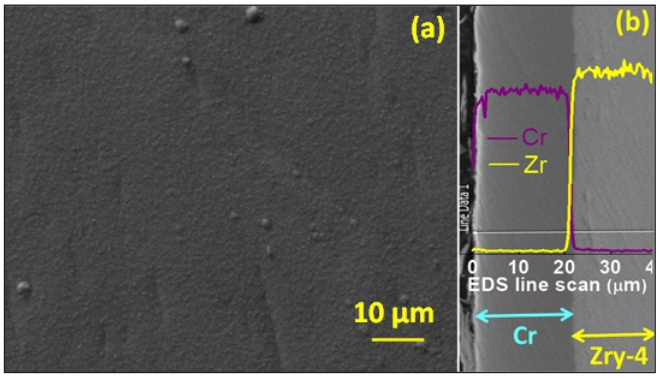

Fig.5: (a) FESEM surface topography of as deposited Cr coating on Zry-4 and (b) cross-section of the Cr/Zry-4 coupons showing uniformity and EDS composition line scan.

into columnar grain structure along the growth axis at higher thickness. No flaking or peeling of the coating was observed throughout the surface.

Presence of residual stress especially tensile stress in high thickness sputter deposited coatings is inevitable and adhesion with substrate becomes a genuine issue. In order to confirm the quality of adhesion of Cr on Zry-4, micro-scratch adhesion test was performed on Cr-coated (20 μm) coupons using Rockwell diamond indenter having radius of 200 μm with loading rate of 30 N.min^{-1}, maximum load of 40 N and a track length of 3 mm using M/s Rtec Instruments micro-scratch tester. The deposited Cr coating exhibited strong adhesion to the Zry-4 substrate, as confirmed by the scratch-adhesion test results. Fig.7(a) displays the scratch mark generated with initiation of arc tensile cracks (Lc1) at 15.8 N load, accompanied by simultaneous acoustic noise and changes in the coefficient of friction (not shown here). The Lc1 represents initiation of cohesive failure. As the normal load increased, the penetration depth increased accompanied by appearance of dense conformal cracks along the loading direction. However, there was no evidence of chipping or delamination of the coating observed up to a load of 40 N, indicating the absence of Lc2. This confirms excellent adhesion of Cr coating with Zry-4 substrate. The maximum scratch groove depth attained was 11.8 μm as confirmed by 2D-optical profilometer image (Fig.7(b)) which further indicates absence of delamination of coating. It was further confirmed by EDS composition line scan across the FESEM scratch groove as shown in Fig.7(c) with no evidence of Zr corroborating the optical profilometer image data.

High Temperature Steam Oxidation

Steam oxidation tests were performed on bare as well as full surface Cr-coated Zry-4 coupons, for comparison, in the temperature range 700°C to 1200°C for different durations in a fabricated tubular furnace. A furnace with 100 mm hot zone was used for carrying out steam oxidation experiments. Oxidation rate was determined by measuring the difference in initial and post oxidation weights and initial surface area. Typical images of Cr-coated coupons before and after steam oxidation at different conditions are shown in Table 3. It is evident that bare Zry-4 suffered severe oxidation even at 700°C, 24 h with formation of non-adherent whitish oxide scale. With further rise in temperature, the severity increased and at 900°C, 16 h, the sample was mostly consumed and disintegrated because of extreme corrosion. Similar trend was continued till 1200°C. On the other hand, Cr-coated zircaloy coupons show highly adherent greenish colour chromium oxide scale formation at 700°C, 24 h which turned into

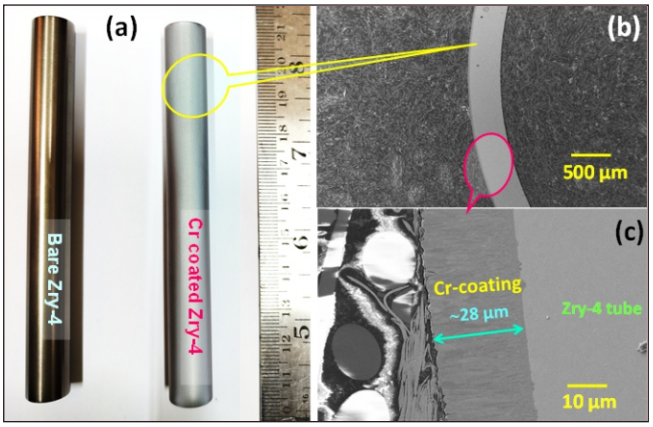

Fig.6: (a) Photographic images of bare and Cr-coated Zry-4 fuel tubes; (b) cross-section FESEM image of Cr-coated Zry-4 tube on OD surface at low magnification and (c) cross-section microstructure of the same at higher magnification.

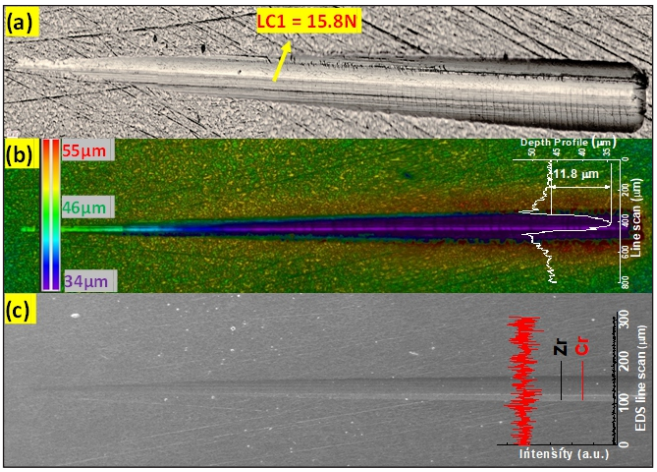

Fig.7: (a) Optical micrograph of the scratch groove generated along the length of the scratch mark; (b) corresponding 2D optical profilometer image showing depth of groove at maximum load of 40 N (11.8 μm) and (c) FESEM image of the scratch groove along with EDS line scan at maximum load 40 N confirming presence of Cr only and absence of adhesive failure.

greenish black at 900°C, 16 h to black at 1200°C, 30 min. retaining the coupons shape. The nature of oxide layer formed on the Cr coating was further analyzed by GIXRD as shown in Fig.4(b). The observed peaks are matching well with Cr_2O_3 oxide structure as confirmed from PCPDF Card No. 38:1479.

This kind of visual observation qualitatively indicates Cr coating indeed provides protection of underneath Zry-4 against steam oxidation till 1200°C for 30 min. In case of Cr-coated sample oxidized at 900°C, 16 h, a slight dimensional distortion could be visible due to edge effect. Sputtering being a line-of-sight process, the nature of coating and its thickness at the edges may not be identical to that on flat surfaces. As a result, the oxide layer touched the beneath zircaloy substrate at the edges and promoted Zry-4 oxidation via oxygen diffusion across the Cr_2O_3 layer and hence the resulting dimensional distortion. However, one can easily address such thickness uniformity issues utilizing multiple gun sputtering system with modified sample holder.

For comparison, the weight gain for both oxidized bare and oxidized Cr coated Zry-4 coupons was compared as shown in Fig.8. At 700°C, 24 h, the weight gain was 59.55 mg.dm^{-2} and 2003 mg.dm^{-2} for Cr-coated Zry-4 and bare Zry-4 respectively. That means Cr-coated Zry-4 showed 33 times less oxidation

Table 3: Photographic images of bare and Cr-coated Zry-4 coupons before and after steam oxidation at different conditions.

Before Steam oxidation	Sample Description	After steam oxidation			
		700°C/24h	900°C/16h	1000°C/3h	1200°C/0.5h
	Cr coated Zry-4	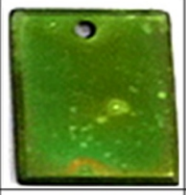			
	Bare Zry-4		Completely disintegrated		

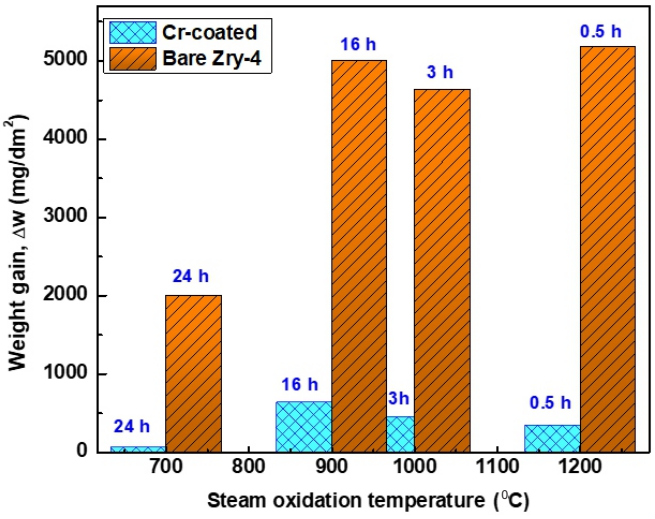

Fig.8: Weight gain vs. steam oxidation temperature histogram plot at different exposure durations.

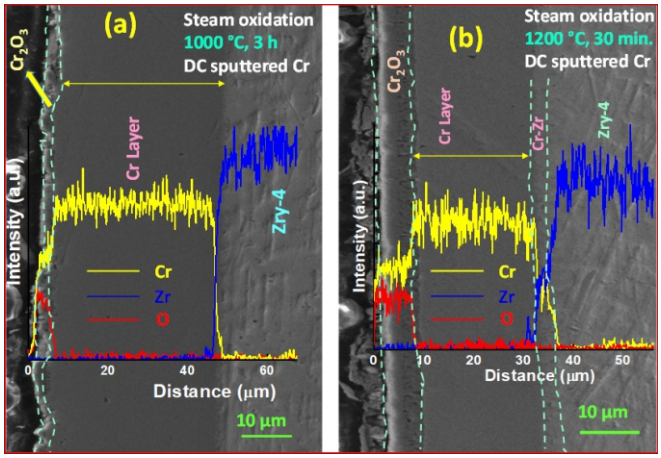

Fig.9: Cross-section FESEM micrographs of steam oxidized Cr coated Zry-4 samples (a) at 1000°C, 3 h; and (b) 1200°C, 30 min. with corresponding EDS composition line scan showing oxide layer as well as unreacted Cr layer thickness, coatings integrity with substrate and Cr diffusion into Zry-4 layer.

than bare Zry-4. At 1200°C, 30 min., under DBA scenario, the Cr-coated Zry-4 with weight gain of 342.78 mg.dm^{-2} exhibited 15 times less oxidation than bare Zry-4 with weight gain of 5174.15 mg.dm^{-2}. These results corroborate the previous literature data on steam oxidation [12, 69-71]. We note that while transferring the bare oxidized zircaloy-4 samples there was loss of ZrO_2 powdery scale depending upon the extent of oxidation and hence the measured weight gain could be lower than the reported data. Careful analysis of the weight gain histogram reveals that upto 900°C, the oxidation rate is rather slow which converts into very high rate of oxidation from 1000°C onwards for both Cr as well as bare Zry-4. These weight gain results clearly show significant improvement in high temperature oxidation behavior of Cr-coated Zry-4 compared to bare sample.

Cross-section FESEM investigation of the oxidized Cr coated Zry-4 samples at two different temperatures 1000°C and 1200°C are shown in Fig.9(a-b). At 1000°C, 3h, the oxide layer thickness is found to be ~3-4 μm but intact with the underneath Cr layer. EDS composition line scan shows oxygen diffusion is very limited within the Cr layer and the Cr/Zr interface is very sharp indicating absence of Cr interdiffusion within the Zry-4 layer. There is no crack or peel off sign within the oxide layer. Due to enhanced severity of oxidation at 1200°C, the Cr_2O_3 oxide layer thickness was grown to 7-8 μm even at 30 minutes of exposure to steam environment. Very careful observation revealed a bilayer structure into Cr_2O_3 oxide film; one porous oxide layer attached to Cr layer with a non-porous oxide cap at the top but no cracks could be seen throughout the cross-section. But the Cr_2O_3 layer is highly adherent to the Cr layer. EDS composition line scan also supports the visual X-section morphology consisting of 4 layer structure Cr_2O_3/Cr/Cr-Zr/Zry-4 corroborating the results of most the previous investigation [10,12,23]. At the Cr/Zr interface, a small fraction of Cr diffusion into Zry-4 layer could be seen at 1200°C (Fig.9(b)) unlike 1000°C (Fig.9(a)). Insertion of a suitable metallic interlayer such as Mo could stop such Cr interdiffusion into Zry-4 layer. This investigation highlights that even ~10 μm Cr coating may be sufficient to protect the Zry-4 claddings from oxidation during DB LOCA scenario. However, it may be necessary to arrest the Cr diffusion into Zry-4 so that formation of Cr-Zr low melting eutectic (1332°C) can be avoided. This can be a problem for future investigation.

Table 4: Steady state analysis of reactivity load of PHWR 37 pin fuel assembly at zero burnup.

No.	Cr thickness (μm)	k_∞ (ν-TRAC)	ρ(mk) (ν-TRAC)	ρ(mk) (OpenMC)	ρ(mk) (DRAGON)
1	Uncoated (Ref.)	1.12460	0.0	0.0	0.00
2	10	1.11905	-4.41	-4.19	-4.3
3	15	1.11630	-6.62	-6.56	
4	20	1.11355	-8.83	-8.71	-8.5
5	25	1.11082	-11.03	-10.92	
6	30	1.10810	-13.24	-13.13	-12.8
7	35	1.10540	-15.45	-15.10	
8	40	1.10271	-17.66	-17.30	-17.1

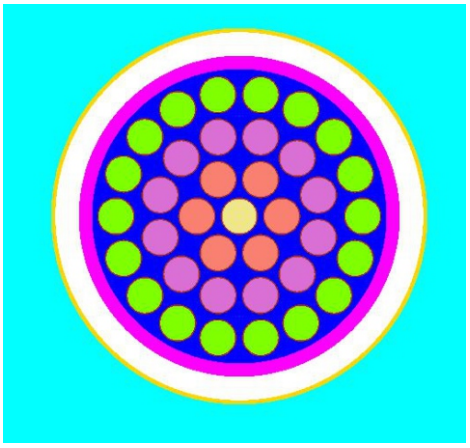

Fig.10: Cross section view of PHWR fuel assembly.

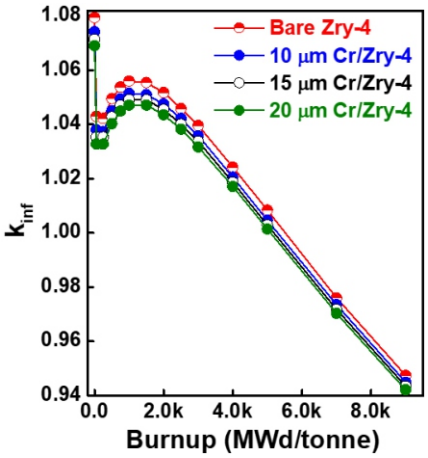

Fig.11: Variation of kinf with burnup for PHWR fuel assembly for different coating thickness.

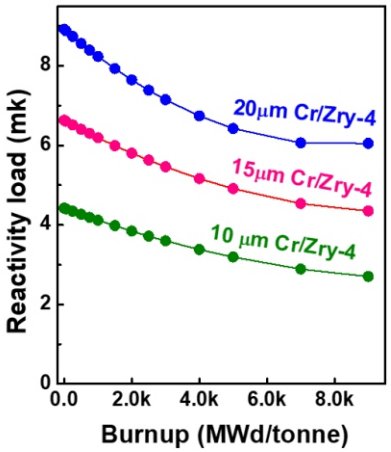

Fig.12: Reactivity load with burnup for 700 MWe PHWR fuel assembly for different thickness of Cr on clad.xidation temperature histogram plot at different exposure durations.

Therefore, this study demonstrates successful deposition of thick (20-30 μm), pore-free and highly adherent Cr coating on Zry-4 coupons as well as Zry-4 PHWR's fuel claddings by DC magnetron sputtering. High temperature steam oxidation of the Cr coated Zry-4 in the temperature range 700°C to 1200°C showed very good protection of underneath Zry-4 claddings even under DB LOCA scenario. This study also envisages that minimum 10-12 μm thick Cr coating may be sufficient to protect Zry-4 claddings from severe steam oxidation by providing enough coping time to the operators during DB LOCA condition.

Theoretical Investigation

Effect of Cr Coating on Nuclear Reactivity in PHWR

Since the thermal neutron absorption cross-section of Cr (2.9 b) is significantly greater than that of Zry-4 (0.22 b), it follows that cladding coated with Cr is likely to adversely affect neutron flux and subsequently core reactivity. An assessment of reactivity effect of Cr coating on the clad outer surface in the context of development of ATF was performed. In this study, the 37 fuel pin PHWR fuel assembly (FA) was analyzed with Cr coating. Calculations were performed using codes ν-TRAC, DRAGON, and OpenMC for different coating thicknesses. Assessment of burnup reactivity load was carried out using DRAGON and OpenMC. Excellent behavior as well as significant advantage of neutron economy has resulted in the use of Zr alloy as the cladding material for most of the thermal reactors operating in the world. However, extensive metal-water reaction in the event of severe accidents and subsequent hydrogen generation is a big disadvantage for Zr alloy. This disadvantage has also resulted in grave consequences both during Chernobyl and Fukushima accidents. Many attempts have been initiated worldwide to find accident tolerant cladding material. One way is to coat the fuel pin clad outer surface with Cr that ensures the safety of fuel in accident scenario by preventing high temperature Zr-water reaction. This study analyzes the reactivity load incurred due to Cr coating of varying thickness on the clad of a 37 fuel pin cluster in a typical PHWR.

Methods and Codes

The results obtained from multiple codes are presented for comparison and benchmarking purposes. Among these, the indigenous lattice transport code ν-TRAC, based on the Method of Characteristics (MOC), is designed for the neutronic analysis of complex heterogeneous lattice cells using ENDF format multigroup cross section data. ν-TRAC has a modular structure, where each module serves a distinct function. The process begins by reading input data and ends with presenting and visualizing lattice results. Further details on the computational methodology are provided in references [72-73]. Additionally, the open source Monte Carlo code OpenMC is also used to compare the results between two codes at zero

burnup. It is based on Monte Carlo method to solve the neutron transport equation. The code analyzes the 3-D fuel assembly geometry using Constructive Solid Geometry (CSG). The inbuilt burnup routine of OpenMC is used to simulate fuel depletion in FA. The FA is simulated as rings of similar burnup, with the power corresponding to 700 MWe PHWR. OpenMC has an inbuilt burnup routine. It is used for burnup analysis in the present study. Thermal scattering is modeled using free gas and thermal scattering law S(α,β) models [74]. Both OpenMC and ν-TRAC utilize the ENDF/B-VII.1 based nuclear data library, in ACE and multigroup format respectively. Further, DRAGON code is also used for calculation using JEFF3.1 library and results are compared in Table 4.

Analysis of Theoretical Results

In this study, a 37 pin cluster of 700 MWe PHWR was analyzed with Cr coating (Fig.10) to assess its impact on the infinite neutron multiplication factor k_∞ and reactivity load (ρ). Table 4 highlights a consistent decrease in k_∞ and corresponding reactivity load with increasing Cr coating thickness. For the uncoated reference, k_∞ was 1.12460 (ν-TRAC). At 10 µm Cr coating, reactivity load was 4.41 mk (ν-TRAC), 4.19 mk (OpenMC), and 4.3 mk (DRAGON), while at 40 µm, it reached 17.66 mk (ν-TRAC), 17.30 mk (OpenMC), and 17.1 mk (DRAGON). As expected, there is an increase in reactivity load with thickness of Cr coating.

Fig.11 illustrates the variation in k_{inf} as a function of burnup for the bare Zry-4 and coated cases with 10, 15 and 20 µm thickness, showing a clear reactivity load from Cr coating throughout the burnup cycle. It is seen from Fig. 12 that the reactivity load due to Cr coating shows a tendency of reduction with burnup. Reactivity load increases with coating thickness, demonstrating a trade-off between reduced neutron multiplication and enhanced accident tolerance. In case of 700 MWe PHWRs, considering a Cr coating thickness of 10 µm on Zry-4 claddings, the reactivity loss is nearly 3 mk as can be seen Fig.12 which is equivalent to typically a burnup loss of ~300 MWd/tonne i.e. 4.28%. With increased thickness of 15 µm, the reactivity loss can be limited to within 5 mk which typically translates as a burnup loss of ~500 MWd/tonne and in terms of percentage ~7.15%. At 20 µm thickness, the percentage loss of burnup turns out to be ~8.92%. That means upto 20 µm Cr coating thickness, the burnup loss can be limited to <10%. These results underline the importance of optimizing Cr coating thickness to achieve a balance between safety and reactivity performance. This kind burnup loss can be negligible in the case of the PHWRs using reprocessed U or fuel with slightly higher content of U^{235}.

Conclusion

A thick (20-30 µm), pore-free highly adherent Cr coating was successfully developed for flat specimen as well as for 100 mm length tubular shape Zry-4 substrates (OD surface) by DC magnetron sputtering. GIXRD and EDS composition analyses confirmed deposition of pure *bcc*-Cr coatings with a sharp Cr/Zry-4 interface as revealed by cross-section FESEM examination. Micro-scratch tests confirmed excellent adhesion of the Cr coating with Zry-4 substrate. The steam oxidation of Cr coated Zry-4 in the temperature range 700-1200°C showed formation of highly adherent protective Cr_2O_3 layer on Cr. Upon steam exposure to 700°C, 24 h, the oxidation rate of Cr coated Zry-4 samples was ~33 times less than bare Zry-4, whereas, at 1200°C, 30 min (DB LOCA condition) the oxidation of Cr/Zry-4 was 15 times less in comparison to bare Zry-4. These experiments have shown that an adherent and compact Cr_2O_3 layer on the Cr acted as an effective barrier for the ingress of oxidizing species. At steam exposure condition of 1200°C, 30 min (DB LOCA scenario), a four layer structure consisting of Cr_2O_3/Cr/CrZr/Zry-4 was formed with 7-8 µm thick protective Cr_2O_3 layer.

The neutron multiplication factor was assessed under cold and hot conditions, both with and without Cr coating. Results for k_∞ from ν-TRAC, OpenMC and DRAGON agree closely at zero burnup. Additionally, the impact of burnup on k_∞ for hot conditions was analyzed for different coating thicknesses. These results highlight the impact of Cr coatings on reducing the multiplication factor of the fuel cluster. Optimal thickness of Cr coating depends on both reactivity load as well as material properties through a comprehensive analysis to achieve a balance between safety and fuel utilization. Considering a thickness of ~15 µm, the reactivity loss can be limited to within 5 mk which typically translates as a burnup loss of 500 MWd/tonne in PHWRs (700 MWe). This study highlights that Cr coating thickness in the range 10-12 µm may be sufficient to protect the Zry-4 claddings under DB LOCA condition with minimum effect on nuclear reactivity in turn burnup loss in 700 MWe PHWRs.

Acknowledgement

Technical support from NAL Bengaluru is highly appreciated.

References

[1] T. R. Allen, R. J. M. Konings, A. T. Motta, Corrosion of Zirconium Alloys, In: R. J. M. Konings, Editor. Comprehensive Nuclear Materials. Oxford, UK, Elsevier, 2012, 49-68.

[2] K. A. Terrani, S. J. Zinkle, L. L. Snead, Advanced oxidation-resistant iron-based alloys for LWR fuel cladding, J. Nucl. Mater., 2014, 448, 420-435.

[3] A. T. Motta, A. Couet, R. J. Comstock, Corrosion of zirconium alloys used for nuclear fuel cladding, Annu. Rev. Mater. Res., 2015, 45, 311-343.

[4] K. A. Terrani, Accident tolerant fuel cladding development: Promise, status, and challenges. J. Nucl. Mater., 2018, 501, 13–30.

[5] C. L. Whitmarsh, Review of Zircaloy-2 and Zircaloy-4 Properties Relevant to N.S. Savannah Reactor Design; ORNL-3281; Oak Ridge National Laboratory: Oak Ridge, TN, USA, 1962.

[6] R. B. Rebak, Accident Tolerant Materials for Light Water Reactor Fuels, Elsevier Book. 2020.

[7] G. Ledergerber, S. Valizadeh, J. Wright, M. Limback, L. Hallstadius, D. Gavillet, et al., Fuel performance beyond design e exploring the limits, in: Top Fuel, 2010, 513-524.

[8] IAEA, Fuel Failure in Normal Operation of Water Reactors: Experience, Mechanisms and Management, IAEA TECDOC 709, IAEA, Vienna, 1993.

[9] Review of Fuel Failures in Water Cooled Reactors, IAEA, Vienna, 2010.

[10] J. Yang, M. Steinbruck, C. Tang, M. Grobe, J. Liu, J. Zhang, S. Yun, S. Wang, Review on chromium coated zirconium alloy accident tolerant fuel cladding, J. Alloy. Compds. 2023, 895, 162450.

[11] Z. Karoutas, J. Brown, A. Atwood, L. Hallstadius, E. Lahoda, S. Ray, J. Bradfute, The maturing of nuclear fuel: Past to Accident Tolerant Fuel. Prog. Nucl. Energy, 2018, 102, 68–78.

[12] C. Tang, M. Stueber, H. J. Seifert, M. Steinbrueck, Protective coatings on zirconium-based alloys as accident-tolerant fuel (ATF) claddings. Corros. Rev., 2017, 35, 141–165.

[13] L. J. Ott, K. R. Robb, D. Wang, Preliminary assessment of accident-tolerant fuels on LWR performance during normal operation and under DB and BDB accident conditions, J. Nucl. Materials, 2018, 448, 520-533.

[14] K. R. Robb, Analysis of the FeCrAl accident tolerant fuel concept benefits during BWR station blackout accidents, Proc. 16th Int. Top. Meet. Nucl. React. Therm. Hydraulics, 2015, 1183-1195.

[15] M. T. Farmer, L. Leibowitz, K. A. Terrani, K. R. Robb, Scoping assessments of ATF impact on late-stage accident progression including molten core-concrete interaction, J. Nucl. Materials, 2014, 448, 534-540.

16) B. J. Merrill, S. M. Bragg-Sitton, P. W. Humrickhouse, Modification of MELCOR for severe accident analysis of candidate accident tolerant cladding materials, Nucl. Eng. Design, 2017, 315, 170-178.

[17] T. Cheng, J. R. Keiser, M. P. Brady, K.A. Terrani, B. A. Pint, Oxidation of fuel cladding candidate materials in steam environments at high temperature and pressure, J. Nucl. Materials, 2012, 427, 396-400.

[18] B. A. Pint, K. A. Terrani, M. P. Brady, T. Cheng, J. R. Keiser, High temperature oxidation of fuel cladding candidate materials in steam-hydrogen environments, J. Nucl. Materials, 2013, 440, 420-427.

[19] B. A. Pint, K. A. Terrani, Y. Yamamoto, L. L. Snead, Material Selection for accident tolerant fuel cladding, Metall. Mater. Trans. E, 2015, 2 (3), 190-196.

[20] H. C. Brassfield, J. F. White, L. Sjodahl, J. T. Bittel, Recommended Property and Reaction Kinetics Data for Use in Evaluating a Light-water-cooled Reactor Loss of Coolant Incident Involving Zircaloy-4 or 304SS Clad UO_2, GEMP-482, General Electric Co., 1968.

[21] J. V. Cathcart, R. E. Pawel, R. A. McKee, R. E. Druschel, G. J. Yurek, J. J. Campbell, et al., Zirconium Metal water Oxidation Kinetics, IV: Reaction Rate Studies, ORNL/NUREG-17, Oak Ridge National Laboratory, 1977.

[22] K. A. Terrani, B. A. Pint, C. M. Parish, C. M. Silva, L.L. Snead, Y. Katoh, Silicon carbide oxidation in steam up to 2 MPa, J. Am. Ceram. Society. 2014, 97, 2331-2352.

[23] M. Steinbrück, N. Ver, M. Große, Oxidation of advanced zirconium cladding alloys in steam at temperatures in the range of 600-1200 °C, Oxid. Met., 2011, 76, 215-232.

[24] D. J. Young, High Temperature Oxidation and Corrosion of Metals, (Elsevier Ltd., Amsterdam, 2016).

[25] N. Birks, G. Meier, and F. Pettit, Introduction to the High Temperature Oxidation of Metals, 2nd ed (Cambridge University Press, Cambridge, 2006).

[26] Outotec, HSC Chemistry 10, (PPORI, 1974–2023).

[27] M. Steinbrueck, M. Grosse, C. Tang, J. Stuckert, H. J. Seifert, An Overview of Mechanisms of the Degradation of Promising ATF Cladding Materials During Oxidation at High Temperatures, High Temp. Corr. Mater., 2024, 101, 621-647.

[28] J. C. Brachet, E. Rouesne, J. Ribis, T. Guilbert, S. Urvoy, G. Nony, C. Toffolon-Masclet, M. Le Saux, N. Chaabane, H. Palancher, A. David, J. Bischoff, J. Augereau, E. Pouillier, High temperature steam oxidation of chromium-coated zirconium-based alloys: Kinetics and process, Corr. Sci., 2020, 167, 108537-15.

[29] D. Kim, H. G. Lee, J. Y. Park, W. J. Kim, Fabrication and measurement of hoop strength of SiC triplex tube for nuclear fuel cladding applications. J. Nucl. Mater., 2015, 458, 29–36.

[30] Y. Katoh, L. L. Snead, C. H. Jr Henager, T. Nozawa, T. Hinoki, A. Ivekovi´c, S. Novak, S. G. De Vicente, Current status and recent research achievements in SiC/SiC composites. J. Nucl. Mater., 2014, 455, 387–397.

[31] X. Zhou, H. Wang, S. Zhao, Progress of SiC_f/SiC composites for nuclear application. Adv. Ceram., 2016, 37, 151–167.

[32] B. Qiu, J. Wang, Y. Deng, M. Wang, Y. Wu, S. Qiu, A review on thermohydraulic and mechanical-physical properties of SiC, FeCrAl and Ti_3SiC_2 for ATF cladding. Nucl. Eng. Technol., 2020, 52, 1–13.

[33] J. Liu, X. Zhang, D. Yun, A complete review and a prospect on the candidate materials for accident-tolerant fuel claddings. Mater. Rev., 2018, 32, 1757–1778.

[34] S. M. Bragg-Sitton, M. Todosow, R. Montgomery, C. R. Stanek, W. J. Carmack, Metrics for the technical performance evaluation of light water reactor accident-tolerant fuel. Nucl. Technol., 2016, 195, 111–123.

[35] H. Chen, X. Wang, R. Zhang, Application and development progress of Cr-based surface coatings in nuclear fuel element: I. Selection, preparation, and characteristics of coating materials. Coatings, 2020, 10, 808.

[36] H. Chen, X. Wang, R. Zhang, Application and Development Progress of Cr-Based Surface Coating in Nuclear Fuel Elements: II. Current Status and Shortcomings of Performance Studies. Coatings, 2020, 10, 835.

[37] B. Cheng, Fuel behavior in severe accidents and Mo-alloy based cladding designs to improve accident tolerance. Atw. Int. Z. Fuer Kernenerg., 2013, 59, 158–160.

[38] A. Nelson, E. Sooby, Y. -J Kim, B. Cheng, S. Maloy, High temperature oxidation of molybdenum in water vapor environments. J. Nucl. Mater. 2014, 448, 441–447.

[39] B. Cheng, P. Chou, Y. -J. Kim, Evaluations of Mo-alloy for light water reactor fuel cladding to enhance accident tolerance. EPJ Nucl. Sci. Technol., 2016, 2, 5.

[40] B. Cheng, P. Chou, Y. -J. Kim, Development of Mo-Based Accident Tolerant LWR Fuel Cladding; International Atomic Energy Agency: Vienna, Austria, 2016.

[41] B. Maier, H. Yeom, G. Johnson, T. Dabney, J. Walters, J. Romero, H. Shah, P. Xu, K. Sridharan, Development of cold spray coatings for accident-tolerant fuel cladding in light water reactors. JOM 2018, 70, 198–202.

[42] J. C. Brachet, T. Guilbert, M. Le Saux, J. Rousselot, G. Nony, C. Toffolon-Masclet, A. Michau, F. Schuster, H. Palancher, J. Bischoff, Behavior of Cr-coated M5 claddings during and after high temperature steam oxidation from 800 °C up to 1500 °C (Loss-of-Coolant Accident & Design Extension Conditions), in: Proceedings of the Topfuel 2018, Prague, Czech Republic, 2018.

[43] X. Han, J. Xue, S. Peng, H. Zhang, An interesting oxidation phenomenon of Cr coatings on Zry-4 substrates in high temperature steam environment, Corros. Sci., 2019, 156, 117–124.

[44] H. -G. Kim, I. -H. Kim, Y. -I. Jung, D. -J. Park, J. -Y. Park, Y. -H. Koo, High-temperature oxidation behavior of Cr-coated zirconium alloy, in: Proceedings of the LWR Fuel Performance Meeting/Topfuel, Charlotte, USA, 2013, 842–846.

[45] Y. Wang, W. Zhou, Q. Wen, X. Ruan, F. Luo, G. Bai, Y. Qing, D. Zhu, Z. Huang, Y. Zhang, T. Liu, R. Li, Behavior of plasma sprayed Cr coatings and FeCrAl coatings on Zr fuel cladding under loss-of-coolant accident conditions, Surf. Coat. Technol., 2018, 344, 141–148.

[46] T. Wei, R. Zhang, H. Yang, H. Liu, S. Qiu, Y. Wang, P. Du, K. He, X. Hu, C. Dong, Microstructure, corrosion resistance and oxidation behavior of Cr-coatings on Zircaloy-4 prepared by vacuum arc plasma deposition, Corros. Sci., 2019, 158, 108077.

[47] Z. Yang, Y. Niu, J. Xue, T. Liu, C. Chang, X. Zheng, Steam oxidation resistance of plasma sprayed chromium-containing coatings at 1200 °C, Mater. Corros., 2019, 70, 37–47.

[48] M. Lenling, H. Yeom, B. Maier, G. Johnson, T. Dabney, J. Graham, P. Hosemann, D. Hoelzer, S. Maloy, K. Sridharan, Manufacturing oxide dispersion-strengthened (ODS) steel fuel cladding tubes using the cold spray process, JOM, 2019, 71, 2868–2873.

[49] J. -M. Kim, T. -H. Ha, I. -H. Kim, H.- G. Kim, Microstructure and oxidation behavior of CrAl laser-coated Zircaloy-4 alloy, Metals, 2017, 7, 59.

[50] J. -M. Kim, T. -H. Ha, J. -S. Park, H. -G. Kim, Effect of laser surface treatment on the corrosion behavior of FeCrAl-coated TZM alloy, Metals, 2016, 6, 29.

[51] C. P. Massey, K. A. Terrani, S. N. Dryepondt, B. A. Pint, Cladding burst behavior of Fe-based alloys under LOCA, J. Nucl. Mater., 2016, 470, 128–138.

[52] X. Li, C. Meng, X. Xu, X. He, C. Wang, Effect of Al content on high-temperature oxidation behavior and failure mechanism of CrAl-coated Zircaloy, Corros. Sci., 2021 192, 109856.

[53] N. Sekido, K. Soeta, K. Yoshimi, Liquidus projection and solidification paths in the Zr-Si-Al ternary system, J. Alloy. Compd., 2021, 885, 160911.

[54] W. Xiao, H. Deng, S. Zou, Y. Ren, D. Tang, M. Lei, C. Xiao, X. Zhou, Y. Chen, Effect of roughness of substrate and sputtering power on the properties of TiN coatings deposited by magnetron sputtering for ATF, J. Nucl. Mater., 2018, 509, 542–549.

[55] M. A. Tunes, F.C. da Silva, O. Camara, C. G. Schön, J. C. Sagás, L. C. Fontana, S. E. Donnelly, G. Greaves, P. D. Edmondson, Energetic particle irradiation study of TiN coatings: are these films appropriate for accident tolerant fuels? J. Nucl. Mater., 2018, 512, 239–245.

[56] E. Alat, A. T. Motta, R.J. Comstock, J. M. Partezana, D. E. Wolfe, Multilayer (TiN, TiAlN) ceramic coatings for nuclear fuel cladding, J. Nucl. Mater., 2016, 478, 236–244.

[57] O. V. Maksakova, R. F. Webster, R. D. Tilley, V. I. Ivashchenko, B. O. Postolnyi, O.V. Bondar, Y. Takeda, V. M. Rogoz, R. E. Sakenova, P. V. Zukowski, M. Opielak, V. M. Beresnev, A. D. Pogrebnjak, Nanoscale architecture of (CrN/ZrN)/(Cr/Zr) nanocomposite coatings: Microstructure, composition, mechanical properties and first-principles calculations, J. Alloy. Compd., 2020, 831, 154808.

[58] A. Michau, F. Maury, F. Schuster, I. Nuta, Y. Gazal, R. Boichot, M. Pons, Chromium carbide growth by direct liquid injection chemical vapor deposition in long and narrow tubes, experiments, modeling and simulation, Coatings, 2018, 8, 220.

[59] J. G. Gigax, M. Kennas, H. Kim, T. Wang, B.R. Maier, H. Yeom, G.O. Johnson, K. Sridharan, L. Shao, Radiation response of Ti2AlC MAX phase coated Zircaloy-4 for accident tolerant fuel cladding, J. Nucl. Mater., 2019, 523, 26–32.

[60] C. Tang, M. Steinbrück, M. Große, T. Bergfeldt, H. J. Seifert, Oxidation behavior of Ti2AlC in the temperature range of 1400 °C–1600 °C in steam, J. Nucl. Mater., 2017, 490, 130–142.

[61] C. Tang, M. Große, S. Ulrich, M. Klimenkov, U. Jäntsch, H. J. Seifert, M. Stüber, M. Steinbrück, High-temperature oxidation and hydrothermal corrosion of textured Cr_2AlC-based coatings on zirconium alloy fuel cladding, Surf. Coat. Technol., 2021, 419, 127263.

[62] P. Richardson, D. Cuskelly, M. Brandt, E. Kisi, Microstructural analysis of in-situ reacted Ti_2AlC MAX phase composite coating by laser cladding, Surf. Coat. Technol., 2020, 385, 125360-8.

[63] Y. Lei, L. Chen, J. Zhang, F. Xue, G. Bai, Y. Zhang, T. Liu, R. Li, S. Li, J. Wang, Influence of Al concentration on mechanical property and oxidation behavior of Zr-Al-C coatings, Surf. Coat. Technol., 2019, 372, 65–71.

[64] Y. Al-Olayyan, G. E. Fuchs, R. Baney, J. Tulenko, The effect of Zircaloy-4 substrate surface condition on the adhesion strength and corrosion of SiC coatings, J. Nucl. Mater., 2005, 346, 109–119.

[65] C. Meng, L. Yang, Y. Wu, J. Tan, W. Dang, X. He, X. Ma, Study of the oxidation behavior of CrN coating on Zr alloy in air, J. Nucl. Mater., 2015, 515, 354–369.

[66] J. Krejčí, J. Kabátová, F. Manoch, J. Kočí, L. Cvrček, J. Málek, S. Krum, P. Šutta, P. Bublíková, P. Halodová, H.K. Namburi, M. Ševeček, Development and testing of multicomponent fuel cladding with enhanced accidental performance, Nucl. Eng. Technol., 2020, 52, 597–609.

[67] J. C. Brachet, I. Idarraga-Trujillo, M. Le Flem, M. Le Saux, V. Vandenberghe, S. Urvoy, E. Rouesne, T. Guilbert, C. Toffolon-Masclet, M. Tupin, C. Phalippou, F. Lomello, F. Schuster, A. Billard, G. Velisa, C. Ducros, F. Sanchette, Early studies on Cr-Coated Zircaloy-4 as enhanced accident tolerant nuclear fuel claddings for light water reactors, J. Nucl. Mater., 2019, 517, 268–285.

[68] F. Qi, Z. Liu, Q. Li, H. Yu, P. Chen, Y. Li, Y. Zhou, C. Ma, C. Tang, Y. Huang, B. Zhao, H. Lu, Pellet-cladding mechanical interaction analysis of Cr-coated Zircaloy cladding, Nucl. Eng. Des., 2020, 367, 110792.

[69] J. C. Brachet, M. Saux, M. Le Flem, S. Urvoy Le, E. Rouesne, T. Guilbert, C. Cobac, F. Lahogue, J. Rousselot, M. Tupin, P. Billaud, C. Hossepied, F. Schuster, F. Lomello, A. Billard, G. Velisa, E. Monsifrot, J. Bischoff J, A. .Ambard, On-going studies at CEA on chromium coated zirconium based nuclear fuel claddings for enhanced accident tolerant LWRs fuel. In: Proceedings of 2015 LWR Fuel Performance/TopFuel, Zurich, Switzerland, September, 2015, 13–19, 31–38.

[70] H. G. Kim, I. H. Kim, Y. I. Jung, D. J. Park, J. Y. Park, Y. H. Koo, Adhesion property and high-temperature oxidation behavior of Cr-coated Zircaloy-4 cladding tube prepared by 3D laser coating. J Nucl Mater., 2016, 465, 531–539.

[71] D. J. Park, H. G. Kim, Y. Jung, J. H. Park, J. H. Yang, Y. H. Koo, Behavior of an improved Zr fuel cladding with oxidation resistant coating under loss-of-coolant accident conditions. J Nucl Mater., 2016, 482, 75–82.

[72] A. Singh, U. Pal, R. Karthikeyan, Evaluation of integral parameters of BAPL and AERE benchmarks using v-TRAC code and ENDF/B VIII.0 library, Nuclear and Particle Physics Proceedings, 2023, 339–340, 78–87.

[73] A. Singh, U. Pal, R. Karthikeyan, V. Harikrishnan, Study of MOX-fueled VVER-1000 pin cell using v-TRAC with ENDF/B-VIII.0 library, Physics Open 2024, 19, 100212.

[74] P. K. Romano, B. Forget, The OpenMC Monte Carlo particle transport code, Ann Nucl Energy, 2013, 51, 274–281.